11th World Congress on Computational Mechanics (WCCM XI)
5th European Conference on Computational Mechanics (ECCM V)
6th European Conference on Computational Fluid Dynamics (ECFD VI)
E. Oñate, J. Oliver and A. Huerta (Eds)

SOLUTION-ADAPTIVE GRID RESOLUTION FOR FLUID STRUCTURE INTERACTION

S. Kneißl[1,2], D. C. Sternel[2], M. Schäfer[2]

[1] Graduate School of Computational Engineering, TU Darmstadt, Dolivostraße 15, 64293 Darmstadt
[2] Institute of Numerical Methods in Mechanical Engineering, TU Darmstadt, Dolivostraße 15, 64293 Darmstadt

Key words: Coupled Problems, Fluid-Structure Interaction, Moving Grid, Grid Adaptivity.

Abstract. We demonstrate a new grid movement strategy, exemplified with a generic fluid-structure interaction (FSI) test case. A flat plate with a prescribed rotational movement in a channel flow is investigated. The transient turbulent flow field is calculated with a low-Re RANS model and two different grid movement methods. Using transfinite interpolation with a grid-point distribution fitted to the stationary starting conditions as grid moving method, leads to errors for the drag-coefficient. By employing a normalized wall distance adaptive method, it is possible to fulfill the near-wall resolution requirements within every time step and thereby getting more accurate results.

1 INTRODUCTION

For many engineering problems the interaction between a moving structure and a turbulent flow is of importance. Numerical models are used to predict the behavior of such systems. The overall solution fidelity strongly depends on the quality of the turbulent flow model used to calculate the forces acting on the structure.
We employ the finite volume method with an URANS (Unsteady Reynolds Averaged Navier Stokes) modeling approach. Here the underlying spatial discretization is decisive for efficiency and accuracy. Furthermore the grid resolution has to fulfill validity requirements implied by the turbulence model in the near wall regions. These are formulated in terms of a velocity normalized wall distance y^+ for the wall adjacent cells.
The need to change the grid that represents the deforming fluid domain, poses a conflict of aims between geometrical cell quality and resolution requirements. Standard techniques for calculating the movement of grid points, like spring analogy methods or interpolation methods (see, for example [1–3]), are designed to keep the initial distribution constant relatively to the structure. These do not address the conflict of aims explicitly and may produce wrong flow solutions if the resolution requirements change.
In this contribution we want show that it is possible to meet the near wall resolution requirements of a RANS model in a generic test case by relocating grid-points according to the flow situation. The idea is, since it is necessary to solve a grid movement problem for the deforming domain anyway, one could also incorporate solution information for a more suited fluid grid. We use the Target-Matrix-Paradigm (TMP) introduced in [5] to formulate the grid movement problem as an optimization problem. It offers the possiblity to express different aspects of cell quality within a uniform principle.
First we present the governing equations that are relevant for computing the turbulent flow fields and understanding why near wall resolution is of interest, then we describe the numerical methods used. After that, the test-case is described and evaluated for a reference grid movement method using transfinite interpolation and the y^+ adaptive movement method.

2 GOVERNING EQUATIONS

For an incompressible Newtonian fluid with constant properties the following equations describe the turbulent mean flow field:

$$\frac{\partial u_i}{\partial x_i} = 0 \quad , \tag{1}$$

$$\rho \left[\frac{\partial u_i}{\partial t} + u_j \frac{\partial u_i}{\partial x_j} \right] = -\frac{\partial p}{\partial x_i} + \frac{\partial}{\partial x_j} [\mu \frac{\partial u_i}{\partial x_j} - \rho \overline{u_i' u_j'}] \tag{2}$$

Where u_i represents the mean flow, p is the mean static pressure, ρ is the density, and μ is the dynamic viscosity. Equation (1) is the continuity equation and equation (2) is the Reynolds averaged Navier Stokes equation. We close the system of equations with the Boussinesq eddy viscosity assumption

$$-\rho \overline{u_i' u_j'} = \mu_t \left(\frac{\partial u_i}{\partial x_j} + \frac{\partial u_j}{\partial x_i} \right) - \frac{2}{3} \rho k \delta_{ij} \tag{3}$$

and two additional transport equations for the turbulent kinetic energy k and the dissipation rate ϵ (Chien [6]):

$$\frac{\partial}{\partial t} (\rho k) + \frac{\partial}{\partial x_j} \left[\rho k u_j - \left(\mu + \frac{\mu_t}{\sigma_k} \right) \frac{\partial k}{\partial x_j} \right] = P - \rho \epsilon - \rho D \tag{4}$$

$$\frac{\partial}{\partial t} (\rho \epsilon) + \frac{\partial}{\partial x_j} \left[\rho \epsilon u_j - \left(\mu + \frac{\mu_t}{\sigma_\epsilon} \right) \frac{\partial \epsilon}{\partial x_j} \right] = (C_{\epsilon_1} P - C_{\epsilon_2} f_1 \rho \epsilon) \frac{\epsilon}{k} + \rho E \tag{5}$$

with

$$\mu_t = C_\mu f_\mu \rho \frac{k^2}{\epsilon} \quad , \tag{6}$$

$$P = \tau_{ij}^{turb} \frac{\partial u_i}{\partial x_j} \quad , \tag{7}$$

$$D = 2\,\nu\, \frac{k}{y^2} \quad , \tag{8}$$

$$E = -\frac{2\nu\epsilon}{y^2} \exp(-0.5 y^+) \quad , \tag{9}$$

$$f_\mu = 1 - \exp(-0.0115 y^+) \quad , \tag{10}$$

$$f_1 = 1 - 0.22 \exp(-\left(\frac{Re_t}{6} \right)^2) \quad . \tag{11}$$

$C_{\epsilon_1} = 1.35$, $C_{\epsilon_2} = 1.8$, $C_\mu = 0.09$, $\sigma_k = 1$ and $\sigma_\epsilon = 1.3$ are model constants. The source terms (8), (9) as well as the damping functions (10), (11) introduce a dependency on the wall distance y^+, which is necessary to make the equation for k and ϵ valid down to the viscous sublayer.

3 NUMERICAL METHODS

3.1 Solving partial differential equations

To solve the above system of partial differential equations we use a finite volume scheme, implemented in our in house code FASTEST [7]. It is a boundary fitted, block structured multigrid solver. The velocity-pressure coupling is achieved via the SIMPLE algorithm. For the time discretization an implicit second order accurate backward differencing scheme is used. The convective fluxes are discretized with the upwind-scheme, whereas the central differencing scheme is used for the diffusive fluxes. The strongly implicit procedure is used to solve the systems of linear equations.

3.2 Grid Movement

To account for the deforming fluid domain we use an optimization approach. In every new time step the movement of the boundary grid points X_b are given by a prescribed motion. Now we want to find displacements for n inner grid points X_i such that an objective function f becomes minimal:

$$\begin{aligned} &\underset{X_i}{\text{minimize}} f(X_i) \\ &\text{where } f(x) : \mathbb{R}^n \to \mathbb{R}, \\ &i = 1, \ldots, n. \end{aligned} \tag{12}$$

We use the target-matrix-paradigm introduced in [5] to formulate a relation $q(X_i)$ between grid points and the quality of the cells they belong to. Here quality is defined as a deviation from an optimal cell. For detailed information see [5]. In the near wall region we define the optimal cells as rectangular and scaled in wall normal direction according to the y+ requirements. In the rest of the field optimal cells are chosen to be just rectangular with an arbitrary size.
The corresponding objective function can be defined as:

$$f\left(X_i\right) = \sum q_i\left(X_i\right) \quad . \tag{13}$$

In order to solve the optimization problem (12) we use the method of steepest descent.
The reference grid distortion method uses a transfinite interpolation to create new inner grid points after the block boundaries have been deformed. See [8] for detailed information.

4 RESULTS AND DISCUSSION

4.1 Description of the test case

As test case we employ a two-dimensional channel flow with a length of 2 m and a height of 0.45 m. In it's center a flat plate with a length of 0.12 m and a height of 0.006 m and rounded edges, which inclines with a constant angular velocity of 175 s^{-1}, serves as obstacle. At the inflow a parabolic profile was chosen to avoid high gradients triggering the refine mechanism at the edges. The Reynolds number based on the channel height and center inflow velocity $u_{max} = 4$ m/s equals $Re = 2.21 \cdot 10^5$. Figure 3 illustrates the setup after 5 ms simulation time. The simulations are started from the stationary non inclined solution.
The starting grid shown in figure 2 is an O-Grid type mesh consisting of 74880 control volumes. The treatment of turbulence in wall proximity as introduced in section 2 is based on the first control volume being located in the viscous sub-layer. Thus y^+ should not exceed 5 and the initial grid has been chosen accordingly as visible from Figure 4d.

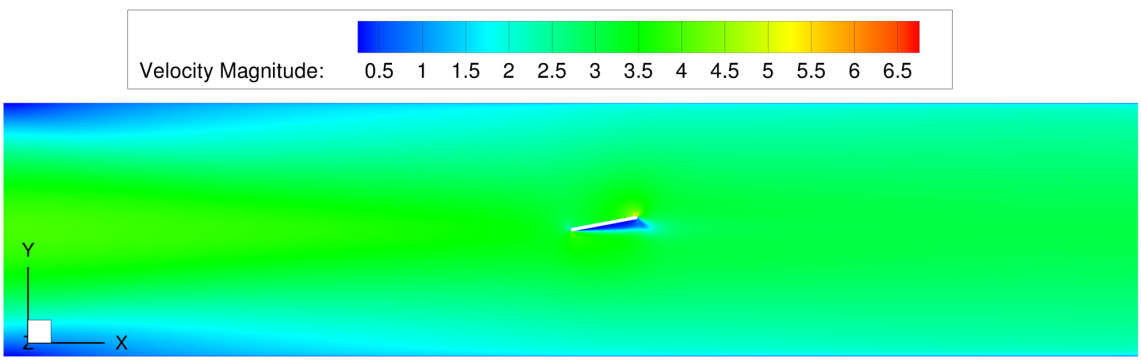

Figure 1: Velocity field in meters per second at $t = 5$ ms

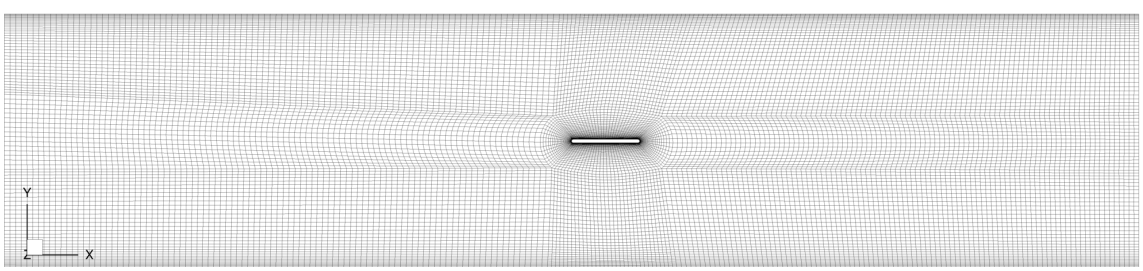

Figure 2: Starting grid

4.2 Evaluation and Discussion

In order to demonstrate that the near wall resolution can be controlled, Figure 4 contains plots of y^+ on the plate's top wall for both methods at different simulation times. The reference method does not change the near wall resolution. So in consequence of the accelerated flow towards the trailing edge the y^+ values surpass the model limit of 5. For the y^+ adaptive method we can not observe a raising tendency.
It has to be mentioned that the exceeding y^+ values could be avoided by choosing a finer initial mesh. But such a trial and error strategy might not be feasible for more complex FSI scenarios.
In order to determine the impact of under-resolved boundary layers on the quality of results, Figure 3 shows both drag coefficients of the plate over time. Clearly, the reference solution produces lower drag forces as the velocity gradients on the wall are not represented correctly.

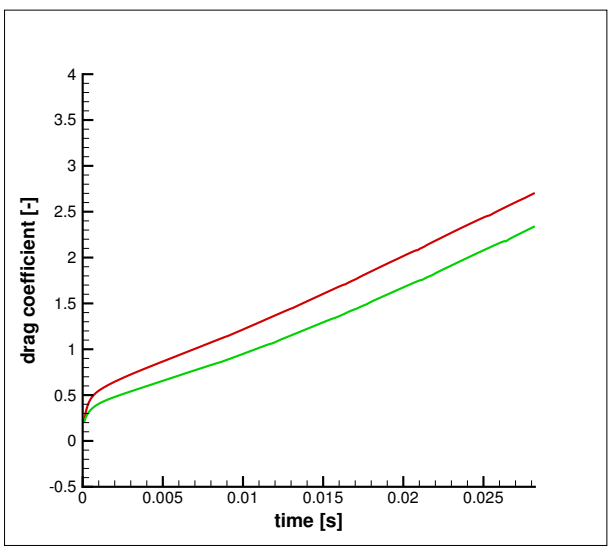

Figure 3: Drag coefficients for adaptive grid movement (red) and for reference grid movement (green) over time

5 Conclusion

We have presented a turbulent test case with prescribed structural motion for which we applied a y^+ adaptive and a non-solution-adaptive grid movement strategy. The conducted numerical experiments showed, that it is important to control the grid resolution for simulations with changing flow conditions as occurring for FSI scenarios. The grid moving strategy outlined in this work in principle is not restricted to just limiting y^+. Other solution dependent criteria are possible as for example velocity gradients aiming to reduce discretization errors.

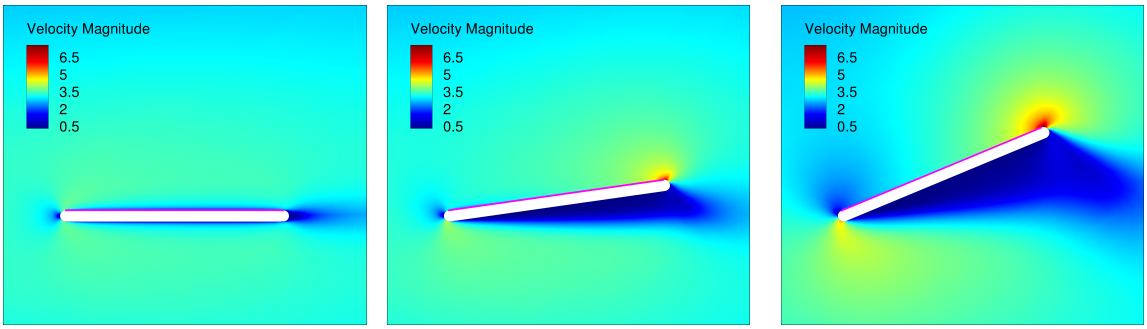

(a) Flow field at $t = 0$ ms (b) Flow field at $t = 7$ ms (c) Flow field at $t = 25$ ms

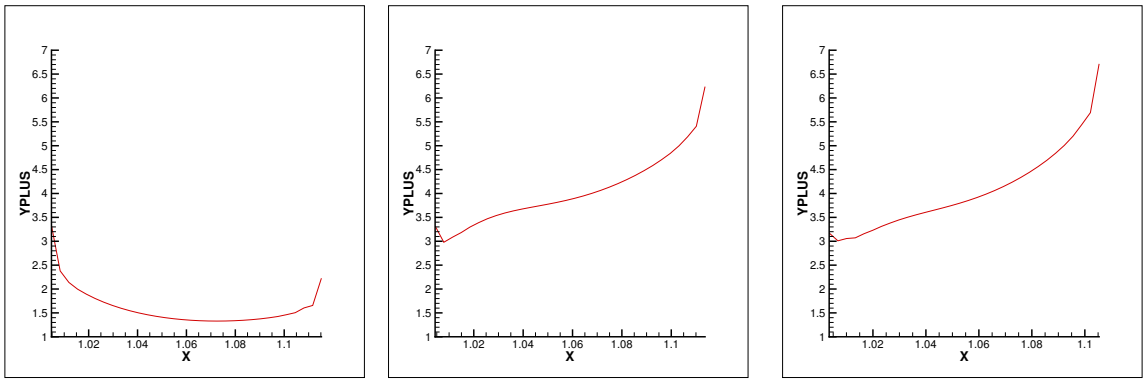

(d) y^+ at $t = 0$ ms for reference grid movement method (e) y^+ at $t = 7$ ms for reference grid movement method (f) y^+ at $t = 25$ ms for reference grid movement method

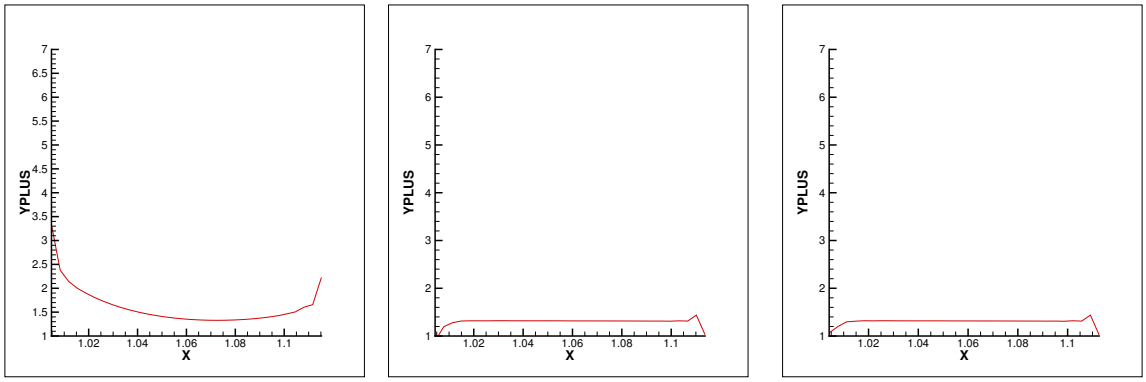

(g) y^+ at $t = 0$ ms for adaptive grid movement (h) y^+ at $t = 7$ ms for adaptive grid movement (i) y^+ at $t = 25$ ms for adaptive grid movement

Figure 4: Comparison of y^+ values on the purple marked lines in a,b,c for different simulation times between the reference grid movement method (d-e) and the y^+ adaptive method (g-i)

ACKNOWLEDGMENT

This work is supported by the 'Excellence Initiative' of the German Federal and State Governments and the Graduate School of Computational Engineering at Technische Universität Darmstadt.

REFERENCES

[1] C. Degand and C. Farhat. A three-dimensional torsional spring analogy method for unstructured dynamic meshes. *Comput. Struct.*, Vol. **80**(3-4), 305-316, 2002.

[2] A. de Boer, M. van der Schoot and M. Bijl. Mesh deformation based on radial basis function interpolation. *Comput. Struct.*, Vol. **85**(11-14), 784-795, 2007.

[3] S. P. Spekreijse, B. B. Prananta an J. C. Kok. A simple, robust and fast algorithm to compute deformation of multi-block structured grid,. *Technical Report - National Aerospace Laboratroy NLR*, NLR-TP-2002-105, 2002.

[4] R.E. Smith. Transnite Interpolation (TFI) Generation Systems. In: Handbook of Grid Generation, eds. N.P. Weatherill, J.F. Thompson, B.K. Soni. CRC Press, 1999.

[5] P. Knupp. Introducing the target-matrix paradigm for mesh optimization via node-movement. *Engineering with Computers.*, Vol. **28**(4), 419-429, 2012.

[6] K.-Y. Chien. , Predictions of Channel and Boundary-Layer Flows with a Low-Reynolds Number Turbulence Model, *AIAA Journal.*, Vol. **20**, No. 1, pp. 33-38, 1982.

[7] Department of Numerical Methods in Mechanical Engineering. FASTEST - User Manual. Technische Universitt Darmstadt, 2005.

[8] P. Pironkov. Numerical Simulation of Thermal Fluid-Structure Interaction. PhD thesis, Technische Universitt Darmstadt, 2010.